Biomacromol. J., Vol. 8, No. 1, 1-9, July 2022.

Biomacromolecular Journal
www.bmmj.org

New Candidates for Furin Inhibition as Probable Treat for COVID-19: Docking Output

M.R. Dayer*

Department of Biology, Faculty of Science, Shahid Chamran University of Ahvaz, Ahvaz, Iran

(Received 5 February 2023, Accepted 14 May 2023)

ABSTRACT

Furin is a serine protease that takes part in the processing and activation of the host cell pre-proteins. The enzyme also plays an important role in the activation of several viruses, such as the SARS-CoV-2 virus, the causative agent of COVID-19 disease which inflicted a high rate of mortality. Unlike other viral enzymes, furin has a constant sequence and active site characteristics and seems to be a better target for drug design for COVID-19 treatment. Considering furin active site as receptor and some approved drugs as ligands, we have carried out docking experiments in HEX software to pick up those which are capable of binding furin active site with high affinity. The tested drugs were chosen from different classes, including antivirals, antibiotics, and anti-protozoa/anti-parasites with suspected beneficial effects on COVID-19. Our docking experiments show that saquinavir, nelfinavir, and atazanavir with respective cumulative inhibitory effects of 2.52, 2.16, and 2.13, respectively are the best candidates for furin inhibition. Clarithromycin, niclosamide, and erythromycin show cumulative inhibitory indices of 1.97, 1.90, and 1.84, respectively. Considering the lower side effects of clarithromycin, niclosamide, and erythromycin in contrast to the antivirals such as saquinavir, nelfinavir, and atazanavir, we suggest the formers as prophylaxes and even at severe states of COVID-19 as adjuvant therapy.

Keywords: Furin, COVID-19, Clarithromycin, Erythromycin, Saquinavir, Nelfinavir

INTRODUCTION

Furin, EC 3.4.21.75, is a 794 residue serine endoprotease that is encoded by the *FURIN* gene. This enzyme belongs to the subtilisin-like proprotein convertase (PC) family that catalyzes the hydrolysis of protein substrates at paired basic residues (Arg-X-(Arg/Lys) -Arg, where X can be any amino acid). The enzyme cuts sections from some inactive or precursor proteins and converts them to their active forms. Furin is ubiquitously expressed in all tissues and is mostly found in the trans-Golgi network [1-3]. Figure 1 represents the primary structure of the inactive form of furin. As it is depicted in figure 1, furin comprises a short signal peptide at the N-terminal followed by a prodomain ending at a cleavage site of R107 upon activation.

The prodomain helps the correct folding of the next catalytic domain initially. This domain inhibits the proteolytic activity of furin until its removal. Therefore, it is also known as an inhibitory propeptide. This domain is cleaved off by autoproteolytics of activated forms of furin or by other subtilisin-like proteases. The next domain is called the catalytic domain, which contains an essential triad of Asp, His, and Ser that take part in proteolytic activity. P-domain is the following domain playing role in regulating enzyme activity at different pH and calcium ion concentrations [4-5]. Cysteine-rich domain (CRD) is the next functional domain ending with the following cleavage site SR683 residues. Under certain conditions, this site is also cleaved off by active

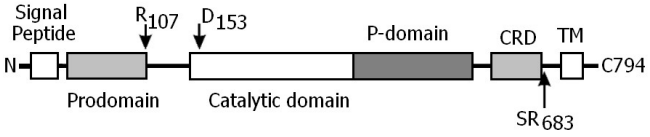

Fig. 1. Primary structure of furin enzyme, includes from N-terminal, signal peptide, prodomain, catalytic domain, p-domain, CRD (cysteine-rich domain), and TM (transmembrane domain), respectively.

*Corresponding author. E-mail: mrdayer@scu.ac.ir

furin or by other subtilisin-like enzymes. Under this condition, furin leeks to the extra cellular compartment with retained activity. The ultimate domain at the C-terminal site of furin is the transmembrane (TM) domain that tightens the enzyme to membranes of the endoplasmic reticulum [6-7].

Besides the physiological role, furin is also recruiting to process some pathogen proteins such as envelope proteins of HIV, influenza, and several filoviruses of Ebola and Marburg virus and also spike protein of SARS-CoV-2 and therefore fully activates the pathogens [8-9]. The tertiary structure of furin, Fig. 2 (left), shows the p-domain beings at the C-terminal part and the catalytic domain being at the N-terminal portion of the protein. Furin catalytic domain, Fig. 2 (right), contains an active site cavity lined with negative charge residues, where the substrates or inhibitors can bind the enzyme and come into contact with the catalytic triad of Asp153, His194, and Ser368 which is important for catalysis. The presence of negatively charged residues in the catalytic site explains the requirement of substrates/inhibitors to carry positive charges for effective binding and also explains the cleavage point of proteins to be at the positive residues of Lys and/or Arg [10-11]. As it is indicated in Fig. 2, there are two or three calcium ions, depending on the origin of furin, that is not involved in the catalytic process but is essential for enzyme native conformation [12-13].

It is well documented that furin is up-regulated in several conditions, like diabetes mellitus, cancer, and viral infections that are suspected to play a role in disease deterioration and so comprise a potential target for drug development and inhibition [14-15]. COVID-19 among the newly emerging viral disease that is caused by SARS-CoV-2 comprises a serious pandemic worldwide with more than 194 million cases and 4.16 million deaths by July 2021. The disease encourages investigators to search for vaccines for healthy individuals or drugs for patients. It is shown that, extra cellular furin plays a critical role in SARS-CoV-2 infectivity [16-17]. The virus uses its surface spike or S protein to bind the host cell receptor called angiotensin-converting enzyme 2 (ACE2). This protein contains an N-terminal (S1) domain, which is responsible for receptor binding, and a C-terminal (S2) domain, for host cell fusion and entrance. Furin by cleaving the spike at the S1/S2 cleavage site accelerates virus entry and pathogenesis [18-20].

One strategy against viral infections is the application of inhibitors against viral enzymes to inhibit viral amplification. The main obstacle in this way is the drug resistance posed by a high rate of replication errors. Inhibition of furin with no drug resistance seems to be a good approach to preventing viral infections especially in the case of COVID-19 [21-22].

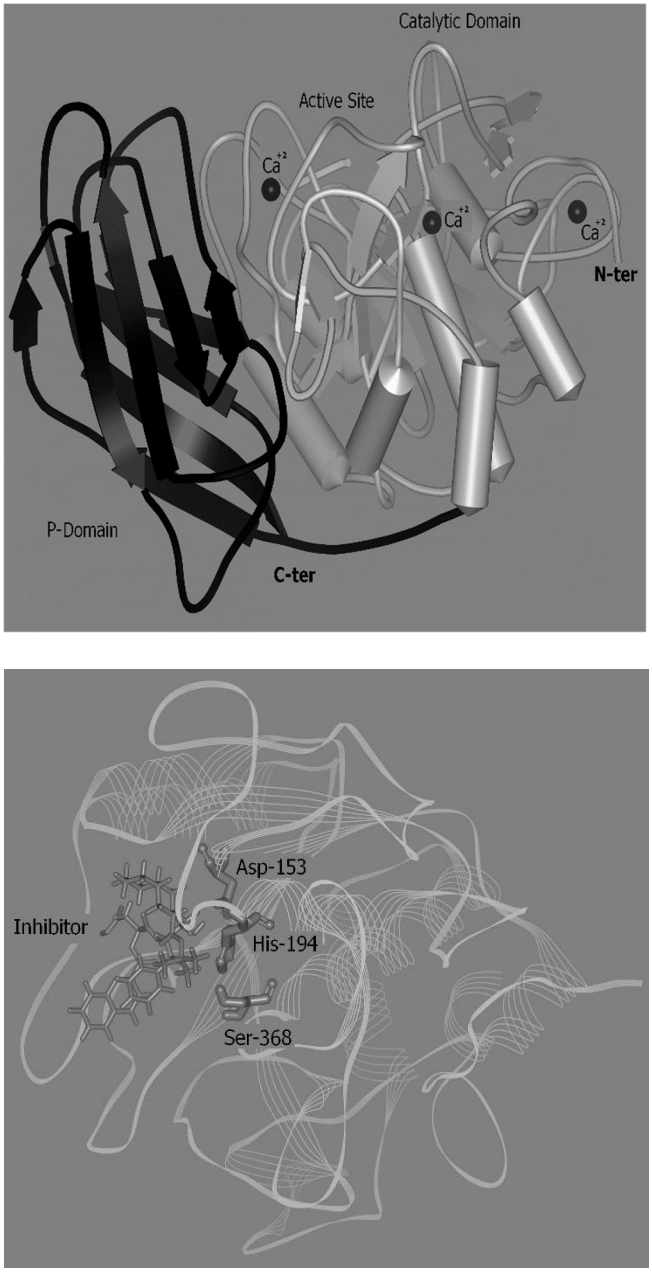

Fig. 2. Above, furin tertiary structure obtained from crystallography studies at 2-angstrom resolutions; Below, furin active site occupied by an inhibitor.

Following this introduction and during this work, we tried to search for drugs capable of binding furin active site and inhibition among known anti-viral and approved antibiotics based on their structural similarities through molecular docking calculations to find and suggest new candidates, which could fight the SARS-CoV-2 virus.

MATERIALS AND METHODS

Furin Coordinate Structure

The coordinate structure of furin with a PDB ID of 4OMD was retrieved from the protein data bank (https://www.rcsb.org/). The structure was obtained by the X-ray diffraction method and refined at the resolution of 2.70 Å. Since the protein structure was refined from dried crystal, its conformation will be far from its native structure in physiological conditions. Accordingly, we optimized and equilibrate the protein structure via minimization to be under 200 kJ mol^{-1} in pH 7.5, 37 degrees centigrade, and 1 atmosphere of pressure using GROMACS 4.5.5 software (http://www.gromacs.org) and GROMOS force field and steepest descent algorithm. The structure was placed in a rectangular box with a dimension of 6.11 × 7.48 × 7.27 nm filled with SPCE water [23-24].

Coordinate Structures of Inhibitors

The chemical structures of candidate inhibitors, including antiviral drugs (amprenavir, atazanavir, baloxavir, darunavir, disoproxil, emtricitabine, indinavir, lamivudine, lopinavir, nelfinavir, nevirapine, oseltamivir, remdesivir, ritonavir, saquinavir, tenofovir, tipranavir, zidovudine) and antibiotics (azithromycin, cefaclor, cefazolin, cefdinir, cefditoren, cefixime, cefotaxime, cefpodoxime, cefprozil, ceftizoxime, ceftriaxone, cefuroxime, ciprofloxacin, clarithromycin, doxycycline, erythromycin, fidaxomicin, gemifloxacin, imipenem, moxifloxacin, ofloxacin, sulfamethoxazole, tetracycline) as well as anti-protozoa/anti-parasite (iminazene, and niclosamide) in SDF format were obtained from PubChem database (https://pubchem.ncbi.nlm.nih.gov/). They were converted to PDB format using Open Babel software (http://openbabel.org/) and their energies were minimized in ArgusLab software (http://www.arguslab.com/) [25].

Furin Active Sites

Furin active site residues, *i.e.* those which are 2 angstroms distant from substrates' atoms inside active site cavity containing catalytic triad of Asp153, His194, and Ser368 were extracted from the PDB structure of 4OMD *i.e.*, the binding site of competitive inhibitor using ArgusLab software (http://www.arguslab.com/) [25]. The active site cavity and its constituents were used to calculate the active site occupations by docked inhibitors.

Molecular Docking Experiments

To carry out molecular docking experiments, the optimized structure of furin with PDBID:4OMD was used as a receptor and the coordinate structure of each inhibitor in PDB formats was used as a ligand for blind docking experiments in Hex 8.0.0 (http://www.loria.fr/~ritchied/hex/) software [26]. The shape + electrostatic and macro sampling modes of docking were used for docking and the best 100 poses and their binding energies were saved for further analysis. The 100 poses then analyzed to calculate the percent of active site occupations for inhibitors and also their binding energies.

Drugs Partition Coefficients

The logP or partition coefficient of a given drug is a known index for hydrophobicity. The more positive values of this coefficient reflect the hydrophobic nature of a chemical, and vice versa [27]. The Virtual Computational Chemistry Laboratory (http://www.vcclab.org/) server was used to calculate logP for each drug [28]. The Simplified Molecular Input Line Entry System (SMILES) for drugs were obtained from PubChem database (https://pubchem.ncbi.nlm.nih.gov/) and subsequently used as input on http://www.vcclab.org/ server to obtain logP.

Data Handling and Analysis

All numerical data were exported to Excel and SPSS software for more analysis. A P-value lower than 0.05 was considered as the significance level.

RESULTS AND DISCUSSION

It is well known that, interruption of S1/S2 cleavage of S protein of SARS-CoV-2 by host protease, especially at furin

```
Wild-Type          6 D--------------------S-----------------------CNCDG     12
                     |                    |                       |||||
PDBID:4OMD       151 DDGKTVDGPARLAEEAFFRGVSQGRGGLGSIFVWASGNGGREHDSCNCDG    200

Wild-Type         13 YTNSIYTLSISSATQFGNVPWYSEACSSTLATTYSSGNQNEKQIVTTDLR     62
                     ||||||||||||||||||||||||||||||||||||||||||||||||||
PDBID:4OMD       201 YTNSIYTLSISSATQFGNVPWYSEACSSTLATTYSSGNQNEKQIVTTDLR    250

Wild-Type         63 QKCTESHTGTSASAPLAAGIIALTLEANKNLTWRDMQHLVVQTSKPAHLN     112
                     ||||||||||||||||||||||||||||||||||||||||||||||||||
PDBID:4OMD       251 QKCTESHTGTSASAPLAAGIIALTLEANKNLTWRDMQHLVVQTSKPAHLN    300

Wild-Type        113 ANDWATNGVGRKVSHSYGYGLLDAGAMVALAQNWTTVAPQRKCIIDILTE     162
                     ||||||||||||||||||||||||||||||||||||||||||||||||||
PDBID:4OMD       301 ANDWATNGVGRKVSHSYGYGLLDAGAMVALAQNWTTVAPQRKCIIDILTE    350

Wild-Type        163 PKDIGKRLEVRKTVTACLGEPNHITRLEHAQARLTLSYNRRGDLAIHLVS     212
                     ||||||||||||||||||||||||||||||||||||||||||||||||||
PDBID:4OMD       351 PKDIGKRLEVRKTVTACLGEPNHITRLEHAQARLTLSYNRRGDLAIHLVS    400

Wild-Type        213 PMGTRSTLLAARPHDYSADGFNDWAFMTTHSWDEDPSGEWVLEIENTSEA     262
                     ||||||||||||||||||||||||||||||||||||||||||||||||||
PDBID:4OMD       401 PMGTRSTLLAARPHDYSADGFNDWAFMTTHSWDEDPSGEWVLEIENTSEA    450

Wild-Type        263 NNYGTLTKFTLVLYGTAPEG-LPVPPESSGCKTLTSSQACVVCEEGFSLH     311
                     |||||||||||||||| .| | ||      :             | | |
PDBID:4OMD       451 NNYGTLTKFTLVLYGTA-SGSL-VP------R-------------G-S-H    477
```

Fig. 3. Sequence alignment result for 4OMD in contrast to its wild-type sequence showing no mutation in 4OMD structure (www.ebi.ac.uk/Tools/psa/emboss_needle/).

site, using inhibitors can prevent virus entry and pathogenesis [28-29]. Accordingly, furin has becomes a good target for drug design against viral infections especially, for the management of the COVID-19 pandemic threat currently [30-31]. Considering the resolved crystal structure of furin, the in silico molecular docking experiments were conducted to predict the ability of some approved drugs as candidates for furin inhibition and their clinical applications for COVID-19 treatment. In confirmation with our hypothesis furin inhibitors that provides therapeutic candidates for multiple disease as COVID-19 either bind to furin active site as competitive inhibitors or to the interface cleft between the P-domain and catalytic site as non-competitive inhibitors [32-33]. Since the binding site seems to be a better target to precisely follow the binding process, in this work we evaluate the binding capacity of the drugs to binding site cavity, and their potential is judged based on their binding energy (-ΔG). To ensure that the selected crystal structure of furin with PDB ID of 4OMD matche the wild-type protein and to survey their uniformity, we performed pair-wise alignment on emboss sever (www.ebi.ac.uk/Tools/psa/emboss_needle/). The 4OMD structure completely has a wild-type structure without any mutations or polymorphisms (see Fig. 3).

Figure 4 represents the binding patterns of drugs to enzyme active site. In this figure only the 10 drugs with more than 40 percent of active site occupation are shown. To have a better representation, those ligands which are binded to other parts of the protein are omitted in this figure.

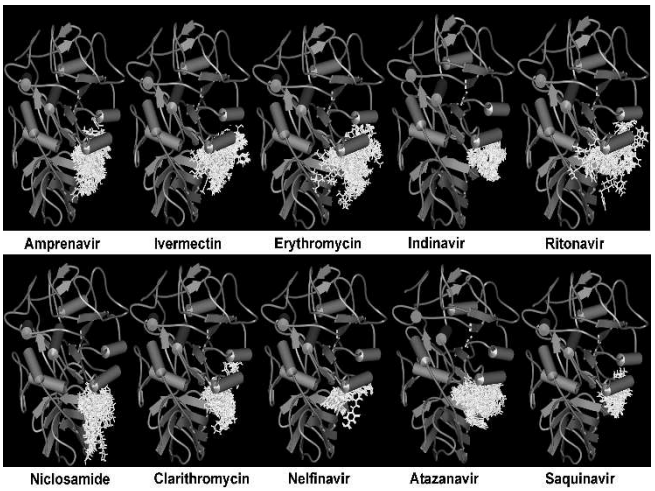

Fig. 4. Docking results for Amprenavir, Erythromycin, Clarithromycin, Niclosamide, Atazanavir, Indinavir, Nelfinavir and Saquinavir extracted from 100 best poses performed in HEX software.

Table 1 represents the docking results including the percent of binding site occupations and the binding energies in kJ mol^{-1} for the considered drugs. Although baloxavir, cefaclor, cefdinir, cefotaxime, cefuroxime, cefpodoxime, ciprofloxacin, emtricitabine, gemifloxacin, imipenem, moxifloxacin, ofloxacin, sulfamethoxazole, and tipranavir could not bind to enzyme active site (0%) and are not considered for further evaluation; but they may bind to an allosteric site and inhibit the enzyme non-competitively. Table 1 also shows the logP for the considered drugs, which reflects the hydrophobicity or bioavailability of drugs to reach the furin as a target for inhibition.

A drug with more hydrophobic (higher logP) and higher binding energy will be a more effective inhibitor. In order to make a reasonable comparison, we normalized the calculated percent of occupation, logP, and binding energy values and summate them in a cumulative index. Therefore, the more cumulative index reveals the more effective drug for furin inhibition.

It is evident that saquinavir, atazanavir, and nelfinavir, obtain a higher score in our series with 2.52, 2.16, and 2.13 cumulative indices, respectively. *In vitro* assays show that, nelfinavir exerts more effects on viral infections in contrast to ritonavir and lopinavir, while there is no experimental evidence regarding the clinical application of atazanavir and saquinavir in viral disease [34-36].

Among the rest anti-viral drugs used in this work, ritonavir, indinavir, amprenavir, remdesivir, lopinavir, nevirapine, darunavir, lamivudine, oseltamivir, zidovudine, and tenofovir with cumulative indices varying between 1.89 to 0.79 retain the next order of effectiveness in furin inhibition. It is important to note that, darunavir has the least affinity to attack furin active site, while it can inhibits furin by binding to its allosteric site high enough, this confirms our finding that darunavir only in 10 percent of probability binds furin active site [37]. Unfortunately, there are no *in vitro* documents for their binding potency for the rest of the selected anti-viral drugs. The obtained results for macrolides used in our study (azithromycin, erythromycin and clarithromycin) with cumulative indices of 0.99, 1.84, and 1.97, respectively reveals that they merit valuable Importance for further studies in the case of COVID-19 treatment; especially in the case of erythromycin and clarithromycin. There are increasing reports regarding the importance of macrolides in COVID-19 treatment [38-40]. Among anti protozoa/parasite drugs used in this work (diminazene, niclosamide, and ivermectin) niclosamide with a cumulative index of 1.90 seems to be a good candidate for

Table 1. Percent of Active Site Occupation, logP Values, and Binding Energies (kJ mol^{-1}) Obtained from Docking Experiments

	% of occupation	logP	Binding energy
Remdesivir	5	2.2	-441.90
Tetracycline	7	-0.56	-362.57
Zidovudine	8	-0.1	-326.77
Darunavir	10	1.89	-348.13
Lopinavir	10	3.91	-280.45
Nevirapine	11	1.75	-383.61
Azithromycin	11	3.03	-401.92
Lamivudine	13	-1.29	-472.23
Oseltamivir	13	1.3	-280.76
Ceftizoxime	14	0.4	-296.96
Cefazolin	15	-0.4	-316.74
Ceftriaxone	20	-0.01	-335.60
Diminazene	20	1.09	-295.01
Tenofovir	20	-1.51	-245.58
Doxycycline	23	-0.72	-328.83
Cefditoren	28	1.7	-357.90
Ritonavir	33	4.24	-359.53
Ivermectin	37	4.04	-277.68
Amprenavir	41	2.03	-347.75
Erythromycin	44	2.37	-382.81
Clarithromycin	47	3.18	-382.47
Niclosamide	47	4.49	-272.53
Atazanavir	51	4.08	-395.35
Indinavir	56	3.26	-273.01
Nelfinavir	62	4.61	-288.81
Saquinavir	86	4.04	-374.82

Table 2. Normalized Values for Active Site Occupation, logP, and Binding Energy in Accordance with the Obtained Cumulative Index

	% of occupation	logP	Energy	Cumulative
Tenofovir	0.23	0.04	0.52	0.79
Cefixime	0.06	0.26	0.67	0.99
Zidovudine	0.09	0.21	0.69	1.00
Tetracycline	0.08	0.16	0.77	1.00
Cefazolin	0.17	0.18	0.67	1.02
Cefprozil	0.03	0.34	0.65	1.02
Ceftizoxime	0.16	0.27	0.63	1.07
Doxycycline	0.27	0.14	0.70	1.10
Oseltamivir	0.15	0.38	0.59	1.13
Ceftriaxone	0.23	0.22	0.71	1.17
Diminazene	0.23	0.36	0.62	1.22
Lamivudine	0.15	0.07	1.00	1.22
Darunavir	0.12	0.46	0.74	1.31
Nevirapine	0.13	0.44	0.81	1.38
Lopinavir	0.12	0.71	0.59	1.42
Remdesivir	0.06	0.50	0.94	1.49
Cefditoren	0.33	0.43	0.76	1.52
Azithromycin	0.12	0.59	0.85	1.57
Amprenavir	0.48	0.47	0.74	1.69
Ivermectin	0.43	0.72	0.59	1.74
Erythromycin	0.51	0.52	0.81	1.84
Indinavir	0.65	0.63	0.58	1.86
Ritonavir	0.38	0.75	0.76	1.89
Niclosamide	0.55	0.78	0.58	1.90
Clarithromycin	0.55	0.62	0.81	1.97
Nelfinavir	0.72	0.79	0.61	2.13
Atazanavir	0.59	0.73	0.84	2.16
Saquinavir	1.00	0.72	0.79	2.52

clinical trial. However, there are reports implying the positive effects of ivermectin in COVID-19 [41-43]. Table 3 summarizes the nature of interaction of drugs with their counterpart residues in the furin active site obtained and analyzed using Protein-Ligand Interaction Profiler (PLIP) server (https://plip-tool.biotec.tu-dresden.de/plip-web/plip/index). This server cinsiders all non-covalent interactions including, hydrogen bonds, salt bridges, hydrophobic interactions etc. for docked complexes. As is evident, all selected drugs make hydrophobic and hydrogen bond interactions with catalytic residues of the enzyme and their neighbors residues that make them effective binders for furin inhibition.

Table 3. Interaction between Drugs Attached to the Furin Active Site Analyzed on the PLIP Server (https://plip-tool.biotec.tu-dresden.de/plip-web/plip/index). H-A (Hydrogen-acceptor Distance) and H-D (Hydrogen-donor Distance)

Inhibitor	Residue	Distance (Angstrom)	Type of interaction
Atazanavir	Leu-227	3.42	Hydrophobic
Atazanavir	Glu-257	3.86	Hydrophobic
Atazanavir	Pro-256	$3.45_{(H-A)}$, $4.06_{(D-A)}$	Hydrogen bond
Atazanavir	Asp-258	$3.06_{(H-A)}$, $3.48_{(D-A)}$	Hydrogen bond
Atazanavir	Asn-295	$3.04_{(H-A)}$, $3.78_{(D-A)}$	Hydrogen bond
Atazanavir	Ser-368	$3.28_{(H-A)}$, $4.05_{(D-A)}$	Hydrogen bond
Nelfinavir	Arg-193	3.79	Hydrophobic
Nelfinavir	Val-231	3.54	Hydrophobic
Nelfinavir	Asp-153	$3.43_{(H-A)}$, $3.89_{(D-A)}$	Hydrogen bond
Nelfinavir	His-194	$2.80_{(H-A)}$, $3.24_{(D-A)}$	Hydrogen bond
Clarithromycin	Asp-191	3.67	Hydrophobic
Clarithromycin	His-194	3.59	Hydrophobic
Clarithromycin	Asp-154	$2.35_{(H-A)}$, $3.32_{(D-A)}$	Hydrogen bond
Clarithromycin	Asp-258	$3.47_{(H-A)}$, $3.99_{(D-A)}$	Hydrogen bond
Clarithromycin	Asp-258	$1.94_{(H-A)}$, $2.88_{(D-A)}$	Hydrogen bond
Clarithromycin	Asp-258	$2.27_{(H-A)}$, $3.07_{(D-A)}$	Hydrogen bond
Clarithromycin	Asn-295	$2.15_{(H-A)}$, $3.12_{(D-A)}$	Hydrogen bond
Clarithromycin	Ser-368	$3.37_{(H-A)}$, $3.87_{(D-A)}$	Hydrogen bond
Erythromycin	Asp-154	3.87	Hydrophobic
Erythromycin	Leu-227	3.60	Hydrophobic
Erythromycin	Trp-254	3.82	Hydrophobic
Erythromycin	Asp-258	3.87	Hydrophobic
Erythromycin	Asp-191	$1.87_{(H-A)}$, $2.75_{(D-A)}$	Hydrogen bond
Erythromycin	Asp-258	4.36	Salt bridge
Niclosamide	Asp-154	3.92	Hydrophobic
Niclosamide	His-194	3.78	Hydrophobic
Niclosamide	Leu-227	3.57	Hydrophobic
Niclosamide	Trp-254	3.90	Hydrophobic
Niclosamidea2	Thr-367	3.40	Hydrophobic
Niclosamide	Leu-227	$1.82_{(H-A)}$, $2.80_{(D-A)}$	Hydrogen bond
Saquinavir	Arg-193	3.74	Hydrophobic
Saquinavir	Leu-227	3.93	Hydrophobic
Saquinavir	Trp-254	3.85	Hydrophobic
Saquinavir	Asp-154	5.13	Salt bridge

CONCLUSIONS

Considering the maximum allowed doses for drugs and their cumulative indices as well as their biocompatibility and side effects, we suggest erythromycin with more than 1 g/day and clarithromycin with 0.4 g/day among macrolides at the first step of disease as prophylaxis over niclosamide (with more than 1 g/day), and antiviral drugs of saquinavir, nelfinavir, indinavir and atazanavir with less than 1 g/day in sever state of the disease with the higher most cumulative indices. Literature surveys indicate to increasing the clinical reports showing the beneficial effects of clarithromycin, niclosamide [44-46] as well as for antivirals of saquinavir, nelfinavir, atazanavir [47-50]. However to the final cure for COVID-19 remain to be confirmed by future studies.

ACKNOWLEDGEMENTS

The author would like to express his thanks to the vice-chancellor of research and technology of the Shahid Chamran University of Ahvaz for providing financial support for this study under Research Grant No: SCU.SB99.477.

REFERENCES

[1] N.G. Seidah, A. Prat, Nat. Rev. Drug Discov. 11 (2012) 367.

[2] A.W. Artenstein, S.M. Opal, N Engl. J. Med. 365 (2011) 2507.

[3] F. Couture, A. Kwiatkowska, Y.L. Dory, R. Day, Expert. Opin. Ther. Pat. 25 (2015) 379.

[4] J.A. Villefranc, S. Nicoli, K. Bentley, M. Jeltsch, G. Zarkada, J.C. Moore, H. Gerhardt, K. Alitalo, N.D. Lawson, Development 140 (2013) 1497.

[5] J. Zhao, W. Xu, J.W. Ross, E.M. Walters, S.P. Butler, J.J. Whyte, L. Kelso, M. Fatemi, N.C. Vanderslice, K. Giroux, L.D. Spate, M.S. Samuel, C.N. Murphy, K.D. Wells, N.C. Masiello, R.S. Prather, W.H. Velander, Sci. Rep. 5 (2015) 14176.

[6] A. Preininger, U. Schlokat, G. Mohr, M. Himmelspach, V. Stichler, A. Kyd-Rebenburg, B. Plaimauer, P.L. Turecek, H.P. Schwarz, W. Wernhart, B.E. Fischer, F. Dorner, Cytotechnology 30 (1999) 1.

[7] B. Plaimauer, G. Mohr, W. Wernhart, M. Himmelspach, F. Dorner, U. Schlokat, Biochem. J. 354 (2001) 689.

[8] B. Coutard, C. Valle, X. de Lamballerie, B. Canard, N.G. Seidah, E. Decroly. Antivir. Res. 176 (2022) 104742.

[9] M. Hoffmann, Molecular Cell. 78 (2020) 779.

[10] J. Declercq, W.M. John, Creemers, in Handbook of Proteolytic Enzymes (Third Edition), 2013

[11] S.O. Dahms, K. Hardes, G.L. Becker, T. Steinmetzer, H. Brandstetter, M.E. Than, ACS Chem. Biol. 9 (2014) 1113.

[12] S. Xia, Q. Lan, S. Su, X. Wang, W. Xu, Z. Liu, Y. Zhu, Q. Wang, L. Lu, S. Jiang, Signal Transduct. Target Ther. 5 (2020) 92.

[13] N. Vankadari, J. Phys. Chem. Lett. 11 (2020) 6655.

[14] J.E. Park, K. Li, A. Barlan, A.R. Fehr, S. Perlman, P.B. McCray Jr, T. Gallagher, Proc. Natl. Acad. Sci., USA 113 (2016) 12262.

[15] Q. Wang, Y. Qiu, J.Y. Li, Z.J. Zhou, C.H. Liao, X.Y. Ge, Virol. Sin. 35 (2020) 337.

[16] Y.W. Cheng, T.L. Chao, C.L. Li, M.F. Chiu, H.C. Kao, S.H. Wang, Y.H. Pang, C.H. Lin, Y.M. Tsai, W.H. Lee, M.H. Tao, T.C. Ho, P.Y. Wu, L.T. Jang, P.J. Chen, S.Y. Chang, S.H. Yeh, Cell Reports 33 (2020) 108254.

[17] M. Hoffmann, H. Kleine-Weber, S. Schroeder, N. Krüger, T. Herrler, S. Erichsen, T.S. Schiergens, G. Herrler, N.H. Wu, A. Nitsche, M.A. Müller, C. Drosten, S. Pöhlmann, Cell. 181 (2020) 271.

[18] M. Yi, Q. Liu, SN Compr. Clin. Med. 2 (2020) 1103.

[19] Y. Adu-Agyeiwaah, M.B. Grant, A.G. Obukhov, Cells 9 (2020) 2528.

[20] S.O. Dahms, M. Arciniega, T. Steinmetzer, R. Huber, M.E. Than, Proc. Natl. Acad. Sci. USA. 113 (2016) 11196.

[21] N.G. Seidah, A. Prat, Nat. Rev. Drug Discov. 11 (2012) 367.

[22] B. Coutard, C. Valle, X. de Lamballerie, B. Canard, N.G. Seidah, E. Decroly, Antiviral Res. 176 (2020) 104742.

[23] C. Sheng, H. Ji, Z. Miao, X. Che, J. Yao, W. Wang, G. Dong, W. Guo, J. Lü, W. Zhang, J. Comput. Aided Mol. Des. 23 (2009) 75.

[24] G. Macindoe, L. Mavridis, V. Venkatraman, M.D. Devignes, D.W. Ritchie, Nucleic Acids Res.

38 (2010) 445.
[25] C. Abdelouahab, B. Abderrahmane, J. Comput. Sci. Syst. Biol. 1 (2008) 81.
[26] D.W. Function, D. Ritchie, S. Vajda, Bioinformatics 24 (2008) 1865.
[27] I.V. Tetko, J. Gasteiger, R. Todeschini, A. Mauri, D. Livingstone, P. Ertl, V.A. Palyulin, E.V. Radchenko, N.S. Zefirov, A.S. Makarenko, V.Y. Tanchuk, V.V. Prokopenko, Aid. Mol. Des. 19 (2005) 453.
[28] B. Coutard, C. Valle, X. de Lamballerie, B. Canard, N.G. Seidah, E. Decroly, Antiviral Res. 176 (2020) 104742.
[29] Q. Wang, Y. Qiu, J.Y. Li, Z.J. Zhou, C.H. Liao, X.Y. Ge, Virol. Sin. 35 (2020) 337.
[30] M. Hoffmann, H. Kleine-Weber, S. Pohlmann, Mol. Cell. 78 (2020) 779.
[31] C. Wu, M. Zheng, Y. Yang, X. Gu, K. Yang, M. Li, Y. Liu, Q. Zhang, P. Zhang, Y. Wang, Q. Wang, Y. Xu, Y. Zhou, Y. Zhang, L. Chen, H. Li, Science 23 (2020) 101642.
[32] G. Thomas, F. Couture, A. Kwiatkowska, Int. J. Mol. Sci. 23 (2022) 3435.
[33] K.P. Devi, M.R. Pourkarim, M. Thijssen, A. Sureda, M. Khayatkashani, C.A. Cismaru, I.B. Neagoe, S. Habtemariam, S. Razmjouei, H.R. Khayat Kashani, Pharmacol. Rep. 74 (2022) 425.
[34] Z. Xu, C. Peng, Y. Shi, Z. Zhu, K. Mu, X. Wang, W. Zhu, bioRxiv 2020.01.27.921627; doi: https://doi.org/10.1101/2020.01.27.921627.
[35] C. Huang, Y. Wang, X. Li, L. Ren, J. Zhao, Y. Hu, L. Zhang, G. Fan, J. Xu, X. Gu, Z. Cheng, T. Yu, J. Xia, Y. Wei, W. Wu, X. Xie, W. Yin, H. Li, M. Liu, Y. Xiao, H. Gao, L. Guo, J. Xie, G. Wang, R. Jiang, Z. Gao, Q. Jin, J. Wang, B. Cao, Lancet 395 (2020) 497.
[36] M.R. Dayer, S. Taleb-Gassabi, M.S. Dayer, Arch. Clin. Infect. Dis. 12 (2017) e13823.
[37] A.J. Gross, Brigham Young U, PhD Dissertation, 2014.
[38] M.A. Gedikli, B. Tuzun, A. Aktas, K. Sayin, H. Ataseven, Bratisl. Lek. Listy. 122 (2021) 101.
[39] A. Yacouba, A. Olowo-okere, I. Yunusa I, Ann. Clin. Microbiol. Antimicrob. 20 (2021) 37.
[40] M.R. Dayer, Org. Chem. Res. 7 (2021) 12.
[41] F.R. Formiga, R. Leblanc, J. de Souza Rebouças, L.P. Farias, R.N. de Oliveira, L. Pena, J. Control Release 329 (2021) 758.
[42] J. Vallejos, R. Zoni, M. Bangher, S. Villamandos, A. Bobadilla, F. Plano, C. Campias, E. Chaparro Campias, F. Achinelli, H.A. Guglielmone, J. Ojeda, F. Medina, D. Farizano Salazar, G. Andino, N.E. Ruiz Diaz, P. Kawerin, E. Meza, S. Dellamea, A. Aquino, V. Flores, C.N. Martemucci, M.M. Vernengo, S.M. Martinez, J.E. Segovia, M.G. Aguirre, Trials 21 (2020) 965.
[43] M.D. Hellwig, A. Maia, Int. J. Antimicrob. Agents 57 (2021) 106248.
[44] K. Tsiakos, A. Tsakiris, G. Tsibris, P.M. Voutsinas, P. Panagopoulos, M. Kosmidou, Petrakis, A. Gravvani, T. Gkavogianni, E. Klouras, K. Katrini, P. Koufargyris, I. Rapti, A. Karageorgos, E. Vrentzos, C. Damoulari, V. Zarkada, C. Sidiropoulou, S. Artemi, A. Ioannidis, A. Papapostolou, E. Michelakis, M. Georgiopoulou, D.M. Myrodia, P. Tsiamalos, K. Syrigos, G. Chrysos, T. Nitsotolis, H. Milionis, G. Poulakou, E.J. Giamarellos-Bourboulis, Infect. Dis. Ther. 10 (2021) 2333.
[45] K. Yamamoto, N. Hosogaya, N. Sakamoto, H. Yoshida, H. Ishii, K. Yatera, K. Izumikawa, K. Yanagihara, H. Mukae, BMJ Open 11 (2021) e053325.
[46] S. Singh, A. Weiss, J. Goodman, M. Fisk, S. Kulkarni, I. Lu, J. Gray, R. Smith, M. Sommer, J. Cheriyan, Br J. Pharmacol. 179 (2022) 3250.
[47] M. Pereira, N. Vale, Biomolecules 12 (2022) 944.
[48] B. Martiniano, M.M. Alberto, B.R. Irving, J. Mol. Model. 26 (2020) 340.
[49] A. Gidari, S. Sabbatini, C. Pallotto, S. Bastianelli, S. Pierucci, C. Busti, E. Schiaroli, D. Francisci, Microorganisms 10 (2022) 2471.
[50] Z. Siami, D. Dehghan, A. Khavandegar, M. Lak, M. Bakhtiyari, Iran. Red Crescent Med. J. 24 (2022) e1576.